COSCH BOOK

http://tinyurl.com/COSCH-book

Chapter [No.8]

Chapter title:
A Study of Spectral Imaging Acquisition and Processing for Cultural Heritage

Authors
Sony George, Jon Y. Hardeberg, João Linhares, Lindsay MacDonald, Cristina Montagner, Sérgio Nascimento, Marcello Picollo, Ruven Pillay, Tatiana Vitorino and E. Keats Webb

One-sentence summary of the chapter:
Due to the increased application of imaging spectroscopy techniques in the cultural heritage field and the consequent diversity of users and usage, a research project was conducted to better understand the instrumentation, the elements of data acquisition, and the effects of the various instruments and methodologies on the accuracy and reliability of the data.

Keywords:
Imaging spectroscopy, polychrome surfaces, reflectance, spectral image quality, image color accuracy, cultural heritage imaging, calibration workflow, multispectral, hyperspectral

1. Introduction

Imaging spectroscopy (IS) techniques, specifically multispectral imaging (MSI) and hyperspectral imaging (HSI), have presented promising advances in the field of non-contact analytical tools for cultural heritage (CH) (Fischer & Kakoulli, 2006; Cucci et al., 2016). The combination of digital imaging with spectroscopy has expanded point-based, or one-dimensional (1D), spectroscopic techniques. IS provides the ability to distinguish and map the spatial distribution of materials over an entire object, extract reflectance spectra for the identification of materials, calculate color, enhance and reveal underdrawings, detect changes in composition, and identify damage and past conservation treatments. The informative potential of these applications and measurements is determined by the characteristics of the acquisition instrumentation. Increased application of IS techniques for the study and documentation of CH has resulted in the development of a range of spectral imaging systems, which are based, for example, on cameras with filtering systems or imaging devices with dispersive elements (MacDonald et al., 2013; Lapray et al., 2014). While the latter can offer better performance in

terms of spectral resolution, they require sophisticated software and operator skills for the handling, processing and interpretation of the large datasets acquired. Along with the variety of systems, procedures such as calibration, if not handled correctly, can make the comparison between the acquired data from different instruments impossible, as well as compromise the reliability of the dataset. The lack of quality metadata collected in a standard way, the insufficiency of a shared common vocabulary, and the heterogeneity of file formats and software are related challenges.

These challenges have been acknowledged and addressed by COSCH Working Group 1 (WG1), which focused on spectral object documentation with the task of identifying, characterizing, and testing spectral imaging techniques and devices in both the visible (Vis, 380-750 nm), near infrared (NIR, 750-1000 nm), and short wave infrared (SWIR, 1000-2500 nm) ranges. To assess the variety of systems and to work towards standardized methodologies and best practices for imaging spectroscopic acquisition of CH, WG1 carried out a Round Robin Test (RRT). Four objects were recorded by nineteen institutions (including museums, research organizations, universities, and IS equipment manufacturers) with various MSI and HSI systems and setups. The RRT was a coordinated effort to gain a better understanding of the instrumentation, the processes of data acquisition, and the effects of the devices and methodology on the reliability of the data. The challenges and issues that arose from bringing different datasets together and understanding the variability seen within them will help to improve protocols for the acquisition, handling, processing and sharing of spectral datasets. The whole experience was focused as a means towards the practical application of non-invasive imaging techniques in the documentation of CH.

This chapter reports some of the most significant results and experiences obtained within COSCH WG1 aimed at the standardization of methods and the promotion of best practices to allow CH professionals to achieve accurate, reproducible and comparable data.

2. Earlier Research

A number of previous efforts have attempted to address colorimetric and spectroscopic imaging methodologies applied to the field of art conservation/documentation. There still exists a significant gap, however, in the standardization of the application of spectral imaging techniques in academic, research and conservation laboratories.

Several projects have contributed to the development of spectral imaging technology for the CH sector and have succeeded in designing high performance hardware and software solutions for accurate image acquisition and processing. These started in the early 1990’s with the VASARI project at National Gallery, London, which achieved accurate high resolution colorimetric documentation of paintings using a filter-based multispectral scanning system in the visible region (Saunders et al. 1993; Martinez et al., 2002). This was later extended in the CRISATEL

project, which extended the work into the NIR and applied basic spectroscopy techniques to the results (Ribés et al., 2005).

Advances in technology made HSI possible in the 2000's and the use of pushbroom imaging spectroscopy was pioneered by IFAC-CNR in Florence (Casini et al., 2005) and by the National Gallery of Art in Washington (Delaney et al. 2010).

Although spectral imaging has been widely accepted by the CH community (Martin et al., 1999; Kerekes & Hsu, 2004; Ribés et al., 2005; MacDonald et al., 2013), there remains a need to define guidelines for accurate image capture and a standardized workflow for processing of the raw data. Spectral image quality is influenced by a number of factors (Shrestha et al., 2014) and understanding their role and how different devices are used in the digital documentation workflow can help better define efficient procedures for acquisition and processing. This has been addressed through the COSCH RRT exercise, as presented in the following sections.

3. COSCH Round Robin Test – Description of work

The RRT involved nineteen institutions acquiring MSI and/or HSI data of four targets. These institutions included museums, research laboratories, universities and hyperspectral equipment manufacturers. Four targets were used for the RRT (Fig. 1): an X-Rite ColorChecker chart, together with its associated white card, a Russian icon, a wavelength standard, and a replica panel painting.

3.1. Round Robin Test

The first RRT object was the traditional standard X-Rite ColorChecker (280 mm x 216 mm) with twenty-four colored square patches, each measuring 40 mm x 40 mm arranged in a four-by-six array. Although the ColorChecker does not fully represent the range of artists' materials or color range, it is, nevertheless, a widely used color reference target within the cultural heritage field and was used to assess and compare the color rendering characteristics of the various imaging devices.

The second object was a 19th century mass-produced Russian icon (265 mm x 220 mm), printed by polychrome lithography, using eight different inks, onto a tinned steel plate and nailed onto a wooden support. It has a glossy surface over the colored areas and a high specular reflectance from the golden metallic surface. The icon was used to investigate the spatial imaging characteristics of IS devices as well as their behavior with highly reflective surfaces.

The third object was a SphereOptics Zenith Polymer Wavelength Standard (90 mm diameter x 15 mm height). Wavelength standards are reflectance targets designed for precise wavelength calibration of spectrophotometers, reflectometers and other spectral instruments. This one is chemically inert, with a diffuse lambertian reflectance, composed of PTFE (Polytetrafluoroethylene) doped with the oxides of the rare earth elements Holmium, Erbium and

Dysprosium. This combination gives the object a stable spectrum of characteristic, well-defined and narrow features over the ultraviolet (UV, 200-380 nm), Vis, NIR, and SWIR spectral ranges, making it very suitable for accurate spectral calibration. The wavelength standard is supplied with traceable, laboratory-certified reference reflectance measurements covering the 200-2500 nm range, and it was used to assess and compare the spectral accuracy of the imaging devices.

Figure 1: a) X-Rite ColorChecker with sampling areas for colorimetric and spectral analysis. b) Russian icon with sampling areas for colorimetric and spectral analysis. c) SphereOptics Zenith Polymer Wavelength Standard. d) Replica panel painting with sampling areas for colorimetric and spectral analysis.

One of the goals of the spectral imaging carried out by the participating groups is the documentation and study of works of art and, in particular, of paintings. The fourth target was, therefore, a painted target created especially for the RRT, made using a classical technique for panel paintings with egg-tempera pigments following the medieval Tuscan painting technique described in Cennino Cennini's 15th century *Il Libro dell'Arte*. The panel (120 mm x 290 mm) consists of a wooden support with a gypsum ground, a canvas layer, and a second gypsum ground layer. Five types of drawing materials (watercolor, charcoal, graphite, a lead and tin-based metalpoint, and a lead-based metalpoint) were used to create lines and line patterns that were then covered with paints applied with two different thicknesses. Seven pigments (carmine, vermilion, burnt umber, malachite, azurite, lead white, and ivory black) were mixed in an egg tempera binder and applied to the panel. They were chosen to have distinctive spectra in the Vis, NIR and SWIR spectral ranges allowing useful spectral analysis to be carried out in any spectral region.

3.2. Methodologies

Imaging spectroscopy is normally classified as either multispectral (MSI) or hyperspectral (HSI) but the distinction between the two is rather blurred (Liang, 2012). The number of bands, their width and continuity are the parameters by which the two techniques differ. MSI systems are designed to acquire images over a limited number of spectral bands, usually with a set of filters having bandwidths from tens to hundreds of nanometers in size. HSI systems acquire images in narrower and more numerous contiguous bands, typically 100 or more. The advantage of HSI systems is to provide almost continuous spectral measurement and therefore they are more accurate than MSI in spectroscopic analysis and material identification (Cucci et al., 2016).

There are several methods of wavelength selection which determine the design of the illumination and the spatial and spectral scanning strategy. For MSI devices tunable light sources may be employed, such as LED-based or filter-based lighting systems, with a monochrome digital camera. Alternatively white light sources may be used with filtered cameras, in which a filter wheel or tunable spectral filters, such as Liquid Crystal Tunable Filters (LCTF) and Acousto-Optical Tunable Filters (AOTF), are placed in front of the sensor (Lapray et al., 2014).

Most of the available HSI systems are based on prism-grating-prism (PGP) line-spectrographs connected to high-sensitivity detectors and the data acquisition is made in pushbroom modality, in which a complete spectrum of each point along a line is formed on one column of the 2D detector array and the area of interest has to be scanned one line at a time. A different HSI technology uses snapshot imaging spectrometers, which collect the entire dataset (or data-cube) in a single integration period without scanning (Hagen et al., 2012). Although the acquisition of a large number of contiguous narrow bands allows an accurate spectral

acquisition, these systems are usually more complex, which decreases their portability and increases their cost.

In Table 1 some of the configurations of the MSI and HSI systems used in the RRT are summarized (Fig. 2).

Figure 2: Different spectral imaging devices used within RRT. Left MSI; right HSI.

The two most important characteristics of MSI and HSI systems are their spatial and spectral resolutions that are linked to their spatial and spectral sampling characteristics. The former is a measure of a system's ability to resolve the desired details in the surface of an object of interest. There are different definitions for the factors related to spatial resolution, including pixel resolution (the number of pixels per linear mm) and optical resolution (the ability of an imaging system to resolve closely-spaced points). Pixel resolution influences the spatial resolution of an image, but is not the only criterion used to evaluate the resolving capabilities of a system. A higher pixel count may increase the image size, but does not guarantee a high spatial resolution, which depends on both optical and electronic components including the lens, aperture, detector and signal processing (Cucci et al., 2016; MacDonald, 2010). The spectral resolution, on the other hand, defines how well the system can resolve the spectral features by sampling wavelength, and is important for material identification (Cucci et al., 2016). Materials can be identified based on their characteristic spectral features, both absorption and reflectance, which can be observed with spectroscopic techniques including IS. Some materials have very narrow spectral features that can only be resolved by systems with a high spectral

resolution, whereas other materials have broader features that can be resolved by systems with a lower spectral resolution.

Table 1- Specification of the imaging devices used in the RRT.

	System Attribute					Set-up information		
	Operative range (nm)	**N° bands**	**Spatial sampling (pix/mm)**	**Spectral sampling (nm)**	**N° Bits**	**Complexity**	**Portability**	**Cost***
MSI LCTF	400-720	33	4.2	1	12	Med	High	M
MSI LCTF	400-720	33	6.8	1	16	Med	High	M
HSI pushbroom	400-900 950-1650	400 332	9-11	1.3 2.1	14	High	Low	E
HSI pushbroom	400-1000	160	16	3.5	14	High	None	E

*Cost: C=cheap (<30,000 €); M=medium (30,000-50,000 €), H=high (50,000-80,000 €) and E=expensive (>80,000€).

3.3. Comparison and evaluation procedures

3.3.1 Colorimetric and spectral analysis

For data comparison a set of areas were selected on the X-Rite ColorChecker and in the Russian Icon (Fig.1a and 1b). At each of these locations spectral reflectance data from the IS systems were averaged and compared with values obtained with a spectro-colorimeter (Minolta CM-2600d) with a d/8° geometry (Fig. 3). For non-uniform surfaces such those of the icon, these measurements may express combinations of rather different spectra. It should also be noted that as the geometry of the spectro-colorimeter is different from that of the imaging systems direct comparison of the results must be done with caution. The CIE L*a*b* coordinates were calculated using the CIELAB 1976 color space with D65 illuminant and 2° standard observer. The CIEDE2000 formula was used to calculate the color (ΔE_{00}) and chroma differences ($\Delta C'$) to compare the acquired and processed data (CIE, 2004).

To compare the reflectance spectra extracted from the data acquired by each device with those acquired with the Minolta, two measures were used: the Root-Mean-Square Error (RMSE) and the Goodness-of-Fit Coefficient (GFC)(Valero et al., 2007). RMSE represents the standard deviation of the differences between two spectra, and GFC represents the cosine of the angle formed by those spectra. The two measures of performance differ since GFC is not affected by scale factors. The value range is from 0 to 100%, with a GFC ≥ 99.5% corresponding to acceptable recovery and GFC ≥ 99.99% to an almost exact fit.

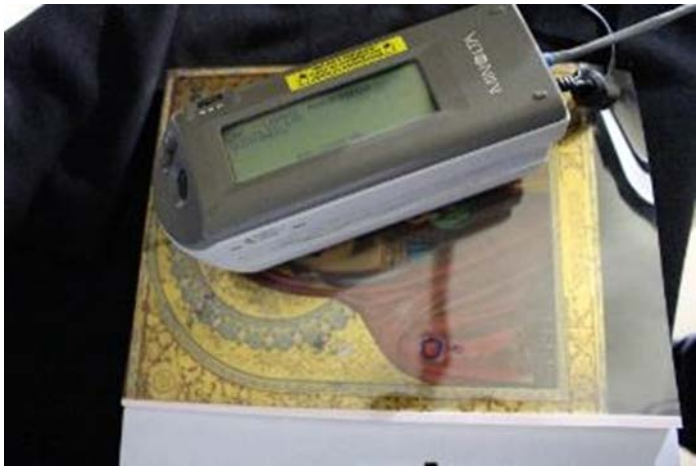

Figure 3: Minolta CM-2600d measuring reflectance spectra on selected areas of the Russian icon.

3.3.2 Spatial Resolution assessment

Spatial resolution may be evaluated using diverse approaches (Holst, 1998). Here three methods for assessing the spatial resolution are presented: visual comparison of resulting images, plotting of vertical profiles, and calculating of the sampling density. The most straightforward way of assessing the spatial resolution of a system is to look at how well the resulting images resolve the details of the documented object. The second way is to plot the vertical profiles of a sequence of high-low reflective materials to determine the contrast between lines and spaces, such as line patterns on the replica panel painting (Fig. 1d). For this object, for instance, as the resolution decreases, the ability to discriminate lines and spaces and the distance between peaks and valleys in the vertical profile plots decreases. The third way is to calculate the sampling density, by dividing the number of pixels between two points by the corresponding physical distance, expressed as pixels/mm.

3.3.3 Spectral alignment accuracy

Spectral alignment accuracy can be obtained by using “spectrally well-known light sources” such as fluorescent lights, xenon or mercury lamps that exhibit distinct and stable spectral features (Polder et al., 2003). An alternative approach is through the use of reflective targets impregnated with rare earth oxides (such as holmium oxide, erbium oxide and dysprosium oxide) that present discrete narrow and strong absorption bands (Burger, 2006). In the RRT a SphereOptics Zenith Polymer Wavelength Standard was used (Fig. 1c).

4. Results for each object

4.1. X-Rite ColorChecker

The ColorChecker was used to evaluate the color and spectral accuracy of the different devices (Fig. 1a). Color differences and other colorimetric parameters calculated from the data acquired

by four participating institutions are presented. Specifically, the discussion on those results is centered on: *i*) the accuracy of color and spectral reproduction of the ColorChecker; *ii*) the problems related to non-homogeneity of the color surface; and *iii*) the definition of the most problematic areas (hues) for accurate color and spectral recording.

Color accuracy was verified by comparing the colorimetric values calculated from the MSI and HSI data with those obtained from direct measurement with the spectro-colorimeter. Figure 4a shows the average ΔE_{00} (black symbols) and $\Delta C'$ (red symbols). Color difference values are in general low and in all case below four units. As expected, systems with a larger number of spectral bands approximate better (Fig. 4a devices 3-4) to the spectrophotometer measurements than those with a small number of bands (Fig. 4a devices 1-2). Comparison of the RMSE and CFG (Figs. 4b and 4c, respectively) suggests that when scale factor is eliminated the performances of both types of systems are very similar.

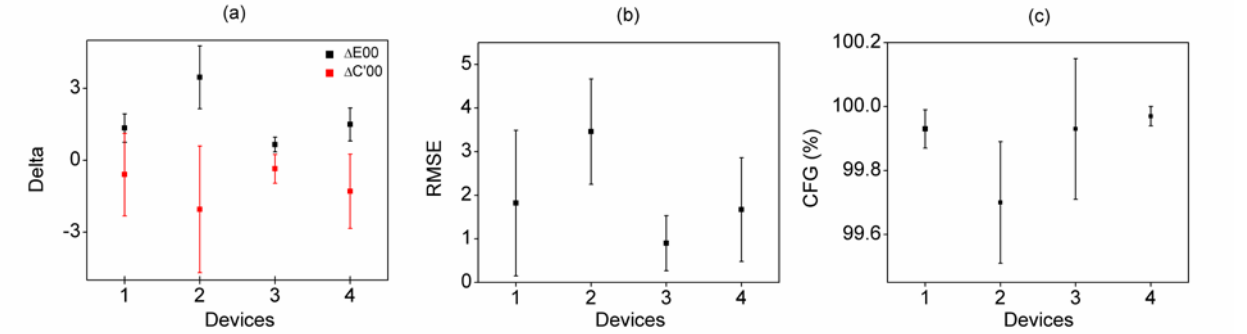

Figure 4: ColorChecker, comparison between the four imaging devices (MSI= 1, 2; HIS= 3, 4) and the spectro-colorimeter measurements: (a) ΔE_{00} and $\Delta C'$, (b) RMSE, and (c) GFC data.

Regarding points *ii)* and *iii)*, the colorimetric comparisons between one MSI and one HSI system against the spectro-colorimeter data across colored samples expressed in ΔE_{00} were also evaluated (Fig. 5). The threshold for color discrimination for human vision is considered 0.3 for uniform samples (Martínez-García et al., 2013), and 3 for image reproduction (FADGI, 2016). In Figure 5, the averaged HSI results show a ΔE_{00} very close to the human limits for color discrimination with the exception of the green (no. 8), red (no. 9), dark skin (no. 19) and foliage (no. 22) areas. The reference data was acquired with a different geometry than the MSI and HSI devices, which can impact the resulting measurements and comparison. Despite the differing geometries, the data acquired from the MSI and HSI devices are consistent with each other and the spectro-colorimeter.

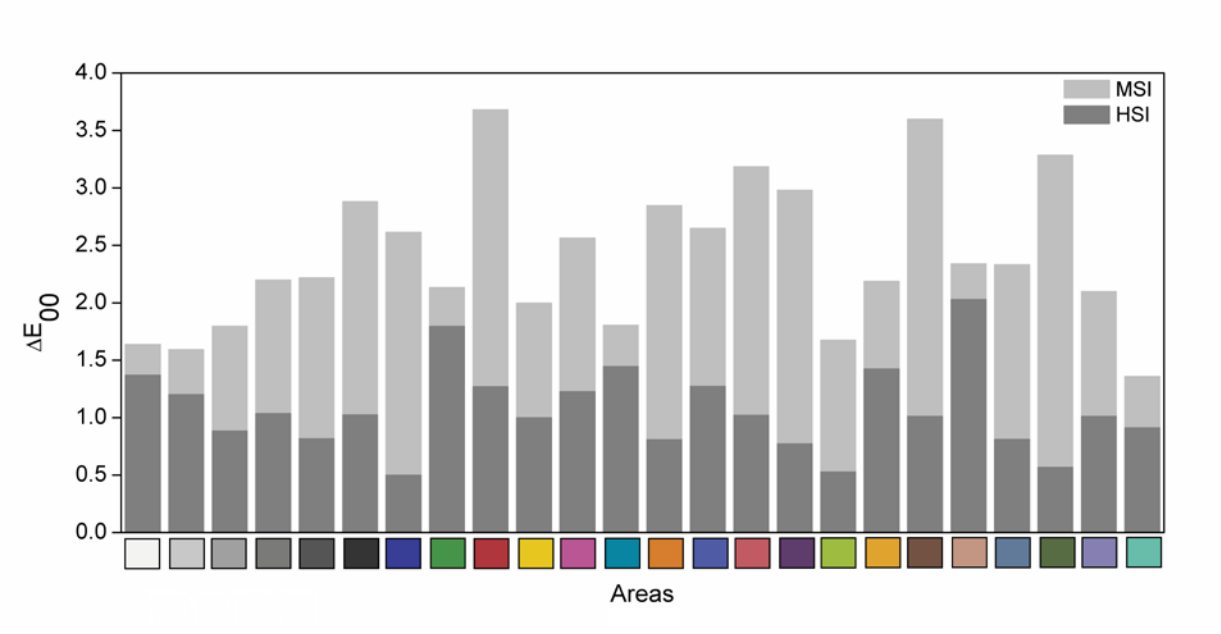

Figure 5: ΔE_{00} for the 24 colored areas of the ColorChecker. Average results for MSI and HSI devices.

4.2. Russian Icon

The Russian icon was selected to establish the imaging performance of systems (Fig. 1b). It was also useful to study the ability of devices to cope with the specular reflectance from its glossy metallic surface.

The results for the Russian icon (Fig. 6) show that the differences, at both spectral and colorimetric levels, between the values extracted from the IS data and those measured with the Minolta spectro-colorimeter are larger than those found with the ColorChecker (Fig. 4). This is a consequence of the fact that the surface of the icon is not diffuse and, here, the measurement geometries of the different devices are critical. However, the differences calculated within this RRT for the Russian icon are still relatively small.

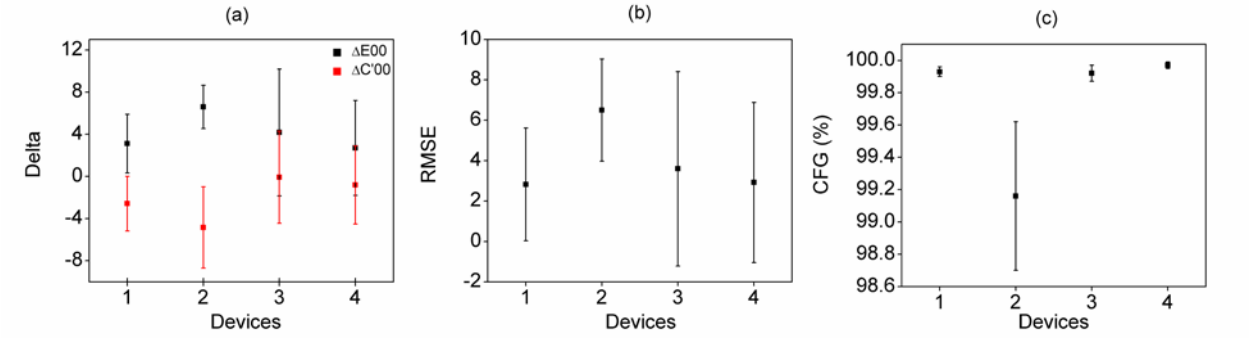

Figure 6: Russian icon, comparison between the four imaging devices (MSI= 1, 2; HIS= 3, 4) and the spectro-colorimeter measurements: (a) ΔE_{00} and $\Delta C'$, (b) RMSE, and (c) GFC data.

The capability to resolve the fine spatial details of the icon also provides an indication of the spatial resolution of each system. An example of a detail extracted from three of the systems is presented in Figure 7.

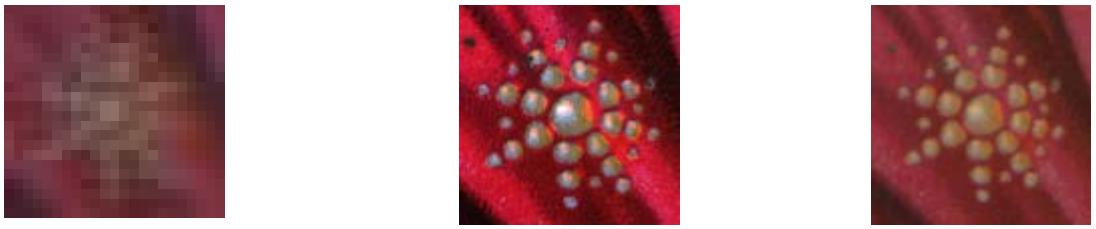

Figure 7: Russian Icon detail extracted from the different devices to show the spatial resolution quality from three IS systems.

The ability of the four IS devices considered here in extracting spectroscopic data from the icon is shown in Figure 8. Through the reported spectra it is fairly evident that there is a sufficiently good accordance among those imaging systems in the obtained spectral shape of the spectra. However, those reflectance spectra cannot be totally superimposed due to differences in their reflectance values across the recorded spectral range. The blue vest and the skin were probably obtained by mixing a white pigment with Prussian blue and a red dye, most likely an anthraquinone-based dye, respectively.

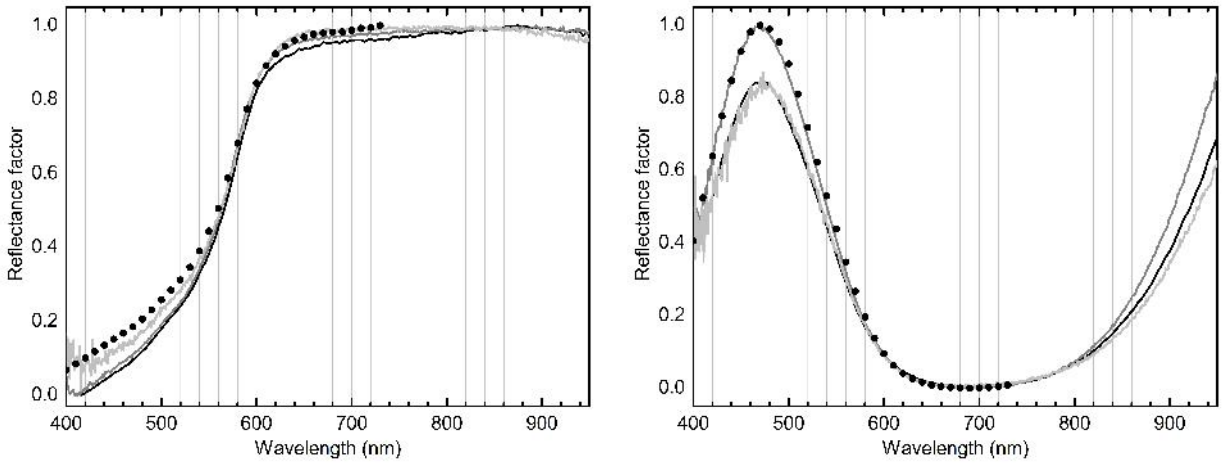

Figure 8: Reflectance spectra from two different colored regions (skin and blue vest, respectively) of the Russian icon reconstructed from the MSI and HSI datasets.

4.3. SphereOptics Zenith Polymer Wavelength Standard

As wavelength standards are designed for use with spectral equipment with high spectral resolution, the analysis in this section is limited to the available data from HSI equipment only. The measured reflectance spectra of the wavelength standard for each HSI system was

determined by taking an average over several thousand pixels, thereby significantly reducing noise. The spectral responses of the different systems for the wavelength standard are shown in Figures 9 and 10, together with the certified reference values for the standard supplied by the manufacturer. The Vis-NIR and SWIR wavelength regions are shown separately. Although, the spectra are broadly similar, there is a clear variability in amplitude, spectral shape and also spectral misalignments between the reference spectra and the calibrated data from the various HSI systems.

The reference standard contains sharp narrow absorption bands and troughs, which in several cases are beyond the spectral resolution of the HSI systems. Each system has slightly different wavelength ranges, different numbers of bands with different central wavelengths and different bandwidths at each wavelength. Therefore, in order to make meaningful quantitative comparisons, it was first necessary to resample each of the acquired data to a common sampling basis and to convolve the reference spectra at the central wavelength for each band with a Gaussian with the camera's given full width half maximum (FWHM) in order to mimic the spectral and bandwidth characteristics of each HSI system. The residual error was calculated for each system from these resampled reference spectra (Fig. 10). Although there are large errors at the sharp bands and troughs, the average errors are relatively small, ranging from 0.005-0.01 in the Vis-NIR region, but much higher in the SWIR region.

The spectral misalignment that can be seen in Figures 9 and 10 can be better visualized by comparing the derivatives of the two spectra. The zero-crossings correspond to the position of the absorption bands and bottoms of the troughs of the reflectance spectra. The results from a single HSI system are shown in Figure 10, where a small spectral misalignment can be clearly seen in the zoomed view. In order to quantify this, phase correlation was used to measure a global offset between the resampled reference signal and the measured spectra. The results in Table 2 show that this spectral misalignment ranged from 0.0-2.6nm in the Vis-NIR region and from 0.0-2.0nm in the SWIR region for the two different HSI systems.

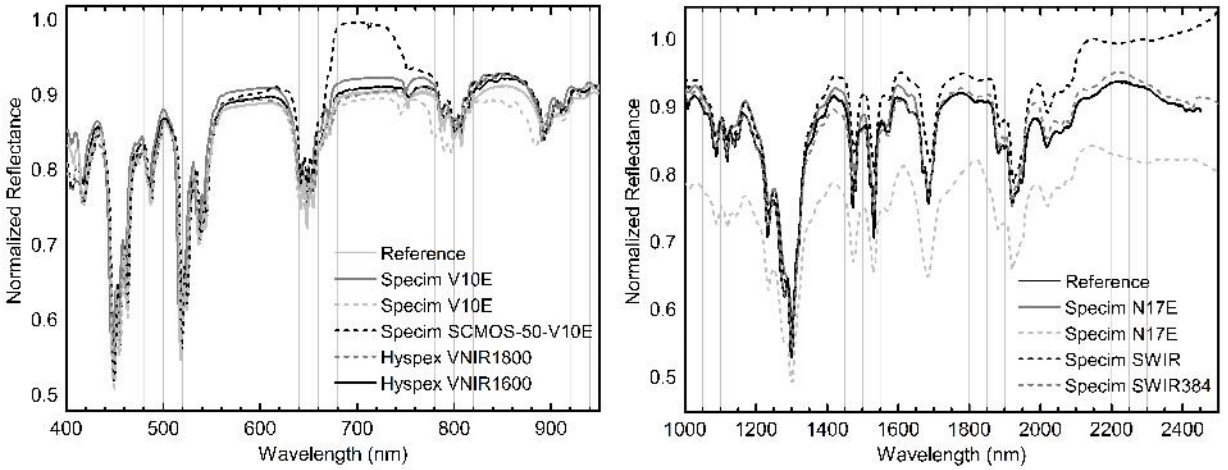

Figure 9: Rare-Earth Wavelength Standard. Comparison of Vis-NIR (left) and SWIR (right) Reflectance.

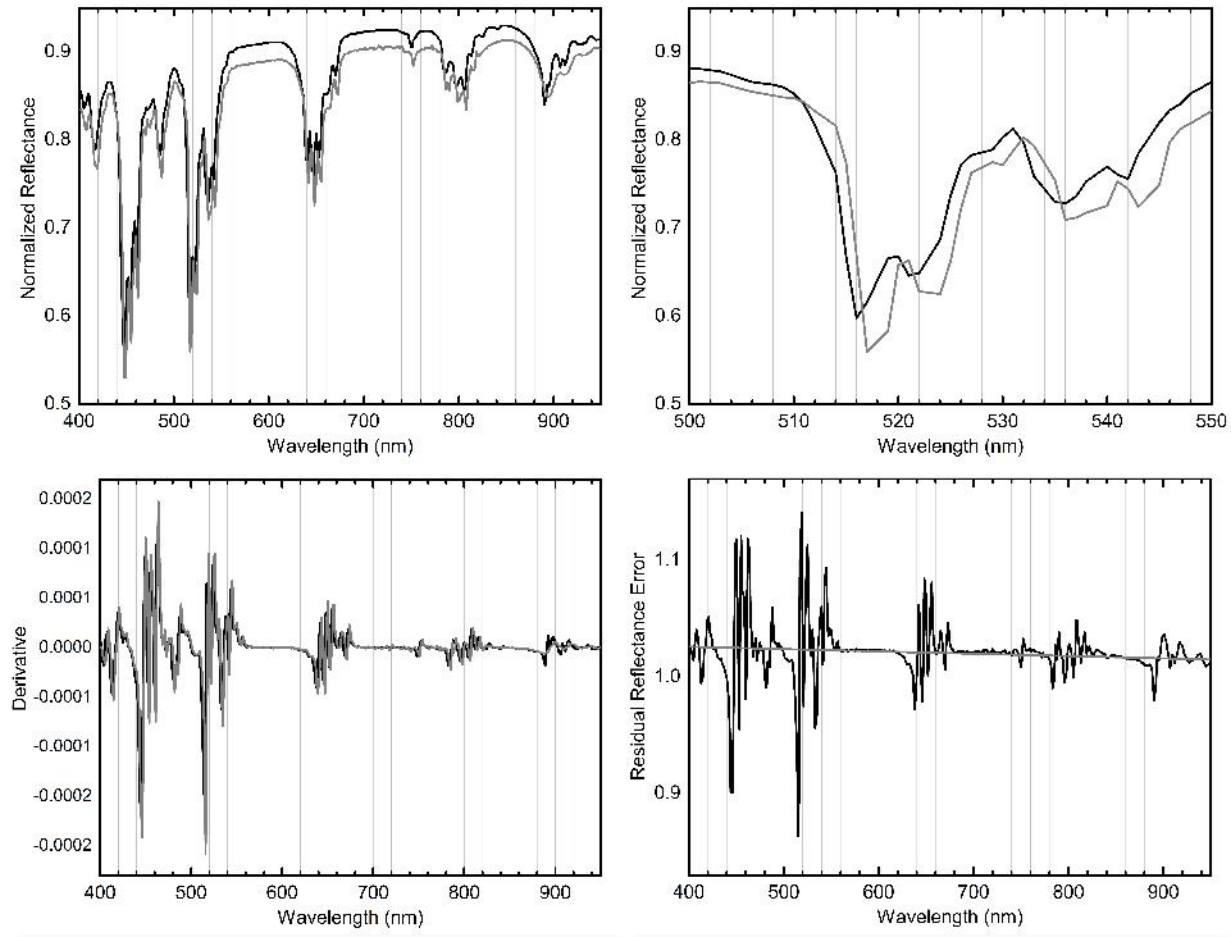

Figure 10: Comparison of the reflectance spectra of wavelength standard for one of the Vis-NIR hyperspectral systems (top left), a zoom of a narrow range of wavelengths showing spectral misalignment (top right), the derivative of the spectra (bottom left) and the residual error with its linear regression (bottom right). Reference = grey line; Vis-NIR hyperspectral system = black line.

Table 2: Spectral misalignment errors of the different devices. One system (*) has very noticeable wavelength-dependent misalignment.

Vis-NIR		SWIR	
System	**Misalignment (nm)**	**System**	**Misalignment (nm)**
Hyspex VNIR1600	0.0	Specim N25E MCT	0.0
Hyspex VNIR1800	-0.1	Hyspex SWIR384 MCT	0.3
Specim V10E	1.0	Specim N25E MCT	0.8
Specim V10E	-1.3	Specim N25E InGaAs	2.0
Specim SCMOS-50-V10E	1.3	Specim N25E MCT	2.0
Specim V10E	2.6*		

4.4. Replica Panel Painting

The replica panel painting was selected to assess the ability of HSI systems to identify and characterize pictorial materials, and their spatial resolution in the NIR-SWIR region to unveil and study underdrawings. Visual comparison of images acquired from the two HSI systems provided an indication of the spatial resolution of the resulting data. As an example, a detail extracted from one of the HSI datasets (Fig. 11) shows how the three sets of watercolor lines with spacing from 2 mm down to 0.5 mm were resolved. The true sensitivity in the spatial resolution of IS devices can be visualized by plotting the vertical profiles of the line patterns on the panel painting. The reported plot of the vertical profiles for the watercolor lines with 2 mm spacing shows a clear differentiation of the lines and spaces with greater distance in amplitudes between the peaks and valleys (Fig. 12).

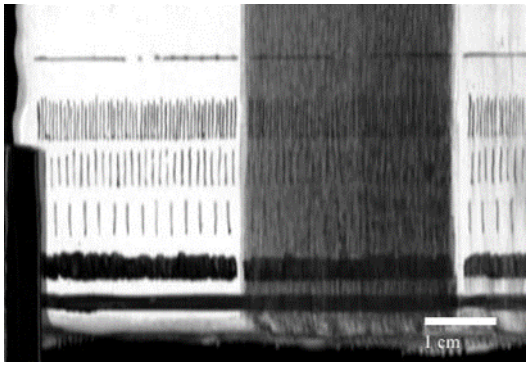

Figure 11: Detail of the replica panel painting extracted at approximately 1040 nm looking at the line patterns to visually assess the system's ability to resolve fine details.

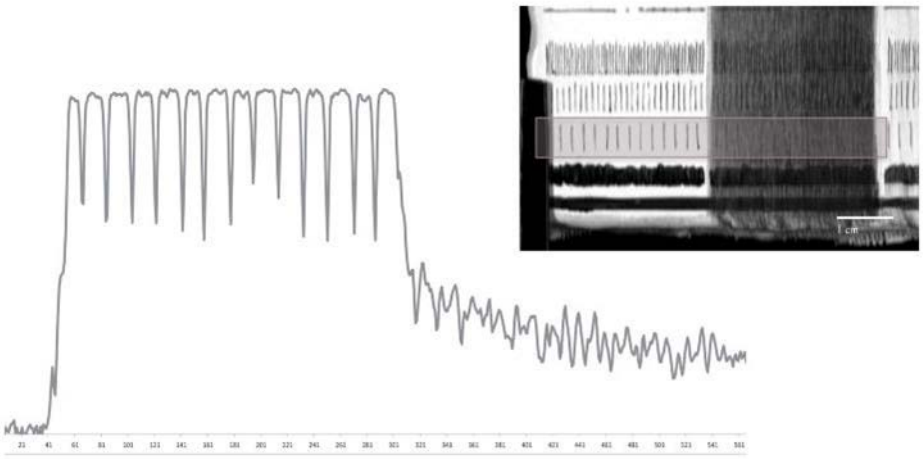

Figure 12: The vertical profile (left) from a HSI device data looking at the exposed watercolor lines (right image) on the test panel. The system is able to differentiate between the lines and spaces as seen with the well-defined peaks.

Concerning the NIR-SWIR region, even if it is possible to discriminate the areas presenting fine details, such as the lines with 1 mm pitch (Fig. 13), the visualization of these underdrawings depends on the transparency of the paint layers. The ability to reconstruct images at different wavelengths from an HSI dataset allows the user to penetrate deeper into the layers and obtain a higher degree of visualization. As an example, for the azurite layer, it was possible to observe the underdrawing clearly at ~1300 nm, and for the malachite layer, the legibility of the lines was only possible at ~1600 nm. For both pigments, IS devices limited to a maximum wavelength of 1000 nm would not have been able to detect underdrawings behind such pigments.

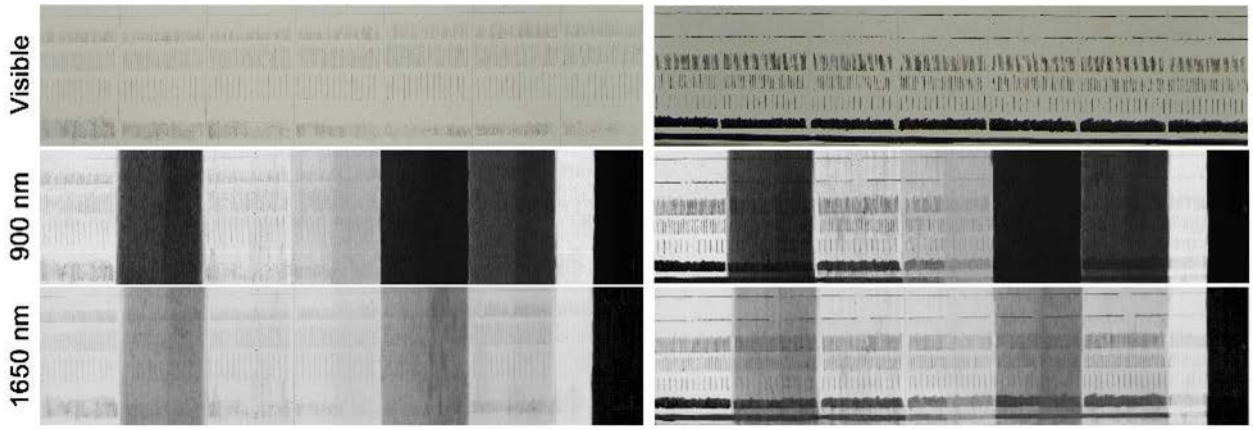

Figure 13. Images extracted from the hyperspectral data-cube at two different wavelengths for the visualization of underdrawing details made with lead- and tin-based metalpoint (left) and watercolor (right) techniques.

Due to the high spatial and spectral sampling of some HSI devices, reflectance spectra from areas of 100 μm or less can be collected on fine polychrome objects. Vis-NIR-SWIR reflectance spectra extracted from the HSI data of the carmine-based red lake, azurite, lead white, and gypsum are reported in Figure 14. In this spectral region gypsum can be identified by its three sub-bands in the 1447-1532 nm range; lead white can be identified by the presence of a spectral feature at 1450 nm; and azurite has its own distinctive absorption band at 1500 nm. Azurite also presents an intense characteristic absorption in the red-NIR region. Spectra of carmine red lake, on the other hand, in the case of paint layers that are less saturated, have a main absorption band in the VNIR structured into two sub-bands at 530±5 nm and 567±3 nm. To identify those spectral bands precisely an IS device with high spectral resolution is usually required.

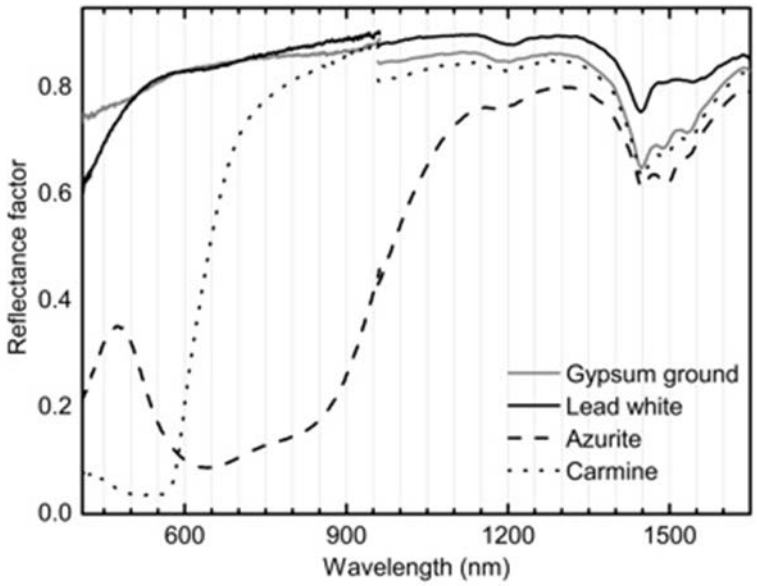

Figure 14: Reflectance spectra from the painted areas made with carmine lake (dotted line), azurite (dashed line), lead white (solid line), and gypsum preparation (grey line) of the replica panel painting.

5. Discussion and Conclusions

The RRT was a coordinated research effort to explore the instrumentation, the differing protocols of data acquisition, and the effects of the instruments and methodology on the accuracy and reliability of the data. It has provided an important insight into the reliability and comparability of IS systems and methodologies in use within the cultural heritage field.

In this chapter, the results of the assessment of a subset of the datasets, consisting of representative MSI and HSI systems has been presented. The results demonstrate that the devices and procedures from the RRT provide broadly consistent results with average color differences at or below accepted thresholds and largely accurate spectral reproduction.

There was, nevertheless, considerable variability in the data. Sources of this variability included the equipment itself (MSI vs HSI, manufacturer, specifications), the users (museums, universities, research laboratories), and the methods of data processing (procedures and workflow), which resulted in varying levels of quality in the final spectral data.
In addition to this, there were several sources of error that affected the resulting data and measurements. These included errors in spectral alignment, noise and distortions including amplitude as well as spatial distortions. Such errors can have important consequences for the use of spectral data in applications such as materials classification or pigment mapping, degradation monitoring and colorimetry.
The results have highlighted the need to work towards standardized methodologies and the need to define best practices. It is important for cultural heritage users to better understand the calibration (spectral, radiometric and spatial calibration) workflow as well as understand the true accuracy, precision and limits of the systems. Improved acquisition protocols and workflows can dramatically improve the accuracy and reliability of the measurements and the resulting data.
In addition, the RRT made clear the importance of regular calibration, validation and testing of the system.
Finally, it is important to stress the interdisciplinary nature of IS methodologies and that their application in the field of cultural heritage requires a blend of inter-disciplinary expertise and collaboration with specialized skill sets and knowledge that contribute to the outcomes of the research and project. This aspect is crucial to obtain satisfactory and reliable results.

Selected Bibliography

Burger, James E., “Hyperspectral NIR Image Analysis – Data Exploration, Correction, and Regression”, Doctoral Thesis No. 60, Swedish University of Agricultural Sciences, 2006.

Casini, Andrea, Bacci, Mauro, Cucci, Costanza, Lotti, Franco, Porcinai, Simone, Picollo, Marcello, Radicati, Bruno, Poggesi, Marco, Stefani, Lorenzo, “Fiber optic reflectance spectroscopy and hyper-spectral image spectroscopy: two integrated techniques for the study of the Madonna dei Fusi,” in Optical Methods for Arts and Archaeology, Munich, Germany, 2005, vol. 5857, p. 58570M–8.

CIE, Colorimetry, CIE Publ.15:2004 (Commission Internationale de L’Eclairage), 2004

Cucci, Costanza, Delaney, John K., Picollo, Marcello, “Reflectance Hyperspectral Imaging for Investigation of Works of Art: Old Master Paintings and Illuminated Manuscripts”, *Accounts of Chemical Research* (2016). DOI: 10.1021/acs.accounts.6b00048.

Delaney, John K., Zeibel, Jason G., Thoury, Mathieu, Littleton, Roy, Palmer, Michael, Morales, Kathryn M., De La Rie, E. Rene´, Hoenigswald, Ann, Visible and infrared imaging spectroscopy of Picasso's Harlequin musician: mapping and identification of artist materials in situ", Appl. Spectrosc. 64(6) (2010): 584-594.

Federal Agencies Digitization Guidelines Initiative (FADGI), "Technical guidelines for digitizing cultural heritage materials creation of raster image files", Ed. Thomas Rieger (2016).

Fischer, Christian, Kakoulli, Ioanna, "Multispectral and Hyperspectral Imaging Technologies in Conservation: Current Research and Potential Applications", *Reviews in Conservation* 7 (2006): 3−16.

Hagen, Nathan, Kester, Robert T., Gao, Liang, Tkaczyk, Tomasz S., "Snapshot Advantage: a Review of the Light Collection Improvement for Parallel High-dimensional Measurement Systems", *Optical Engineering* 51 (2012): 111702.

Holst, Gerald C., "Sampling, Aliasing, and Data Fidelity for Electronic Imaging Systems, Communications, and Data Acquisition", Bellingham WA: SPIE Press, pp.65-97, 1998.

Lapray, Pierre-Jean, Wang, Xingbo, Thomas, Jean-Baptiste, Gouton Pierre, "Multispectral Filter Arrays: Recent Advances and Practical Implementation", *Sensors* 14 (2014): 21626-21659. DOI: 10.3390/s141121626.

Liang, Haida, "Advances in Multispectral and Hyperspectral Imaging for Archaeology and Art Conservation", *Applied Physics A* 106 (2012): 309–323.

Kerekes, John P., Hsu, Su May, "Spectral Quality Metrics for VNIR and SWIR Hyperspectral Imagery." In *Algorithms and Technologies for Multispectral, Hyperspectral, and Ultraspectral Imagery X*, edited by Sylvia S. Shen, Paul E. Lewis, 549-557. Orlando, 2004.

MacDonald, Lindsay W., The Limits of Resolution. Proceedings of Conference on Electronic Visualisation and the Arts (EVA) London, July 2010, pp. 149-156.

MacDonald, Lindsay, Giacometti, Alejandro, Campagnolo, Alberto, Robson, Stuart, Weyrich, Tim, Terras, Melissa, Gibson, Adam, "Multispectral Imaging of Degraded Parchment." In

Computational Color Imaging, edited by Shoji Tominaga, Raimondo Schettini, Alain Trémeau, 143-157. Springer Berlin Heidelberg, 2013.

Martin, L., Vrabel, J., Leachtenauer, J., "Metrics for Assessment of Hyperspectral Image Quality and Utility," in Proceedings of International Symposium on Spectral Sensing Research, Las Vegas, USA, 1999.

Martínez-García, J., Bokaris, P.A., Gómez-Robledo, L., Melgosa, M., "Diferencias de cromaticidad umbrales y supraumbrales mediante fórmulas de diferencia de color avanzadas", in Proceedings X Congreso Nacional del Color, Valencia (Spain), (2013): 503-508, ISBN: 978-84-9048-058-8.

Martinez, Kirk, Cupitt, John, Saunders, David, Pillay, Ruven, "Ten Years of Art Imaging Research", *Proceedings of the IEEE* 90 (2002): 28-41.

Polder, Gerrit, van der Heijden, Gerie W. A. M., Keizer, L. C. Paul, Young, Ian T., “Calibration and Characterisation of Imaging Spectrographs", *Journal of Near Infrared Spectroscopy* 11 (2003): 193-210.

Ribés, Alejandro, Schmitt, Francis, Pillay, Ruven, Lahanier, Christian, "Calibration and Spectral Reconstruction for CRISATEL: an Art Painting Multispectral Acquisition System", *Journal of Imaging Science and Technology* 49 (2005): 463-473.

Saunders, David, Cupitt, John, “Image Processing at the National Gallery: The VASARI Project,” *The National Gallery Technical Bulletin*, vol. 14, pp. 72–85, Jan. 1993.

Shrestha, Raju, Pillay, Ruven, George, Sony, Hardeberg, Jon Yngve, “Quality Evaluation in Spectral Imaging - Quality Factors and Metrics", *Journal of the International Colour Association* 12 (2014): 22-35.

Valero, Eva M., Nieves, Juan L., Nascimento, Sérgio M. C., Amano, Kinjiro, Foster, David H., “Recovering Spectral Data from Natural Scenes with an RGB Digital Camera and Colored Filters”, *COLOR research and application*, Volume 32, Number 5, 2007.